Treatment of shocks with $c = 1$ techniques

Gautam Mandal

BaSM

ICTS, Bangalore, 31 July 2017

Ongoing work with Manas Kulkarni and Takeshi Morita

1D Fluids and shocks

- We will consider unitary nonequilibrium evolution of an one-dimensional gas of fermions. Much of the analysis will go through for a Bose gas in the "Tonks" limit– defined by an infinite strength delta-function replusion.

- Such evolution is experimentally observable in ultra-cold atom systems. *Damski 2006, Calabrese 2013*

- The initial non-stationary state can be developed by a quantum quench (such as a release from a parabolic trap to a periodic box *Caux, Konik 2012*) or by some other method.

- We will consider
(a) production of shock waves
(b) thermalization

- Both have interesting features.

Shock waves

• Analytic treatment using conventional hydrodynamics does not describe shock waves as the equations develop singularities. This is traditionally handled by the addition of various ad hoc terms in the equation (see below), which compare well (*Damski 2006*) with the numerical N-body quantum evolution up to the formation of the shock but fails beyond.

• We show, generalizing earlier work in the context of $c = 1$ matrix model (see later), that
(a) conventional hydrodynamics, in its regime of validity, can be derived from the dynamics of fluid droplets in phase space, and
(b) the droplet dynamics remains valid beyond the formation of any number of shock fronts, which appear in phase space as folds or overhangs.
This is an example of "desingularization" by adopting a higher dimensional description.

• Our treatment does not need ad hoc terms. The phase space evolution equations are derived from a second quantized fermion theory in a classical limit (large N) using the method of coadjoint orbits.

Conventional hydrodynamics and attempted modification

Conventional hydrodynamics: $\rho(x,t)$ fermion density; $\rho(x,t)v(x,t)$

$$\partial_t \rho + \partial_x(\rho v) = 0 \quad \text{Continuity}$$

$$\partial_t v + \partial_x(v^2/2 + \pi^2\rho^2/2 + V(x)) = 0 \quad \text{Euler equation}$$

These equations fail when, at some time t_c and at some point x_c, the density develops a singularity

$$\frac{\partial \rho}{\partial x}|_{t_c,x_c} = \infty.$$

We will call this a shock wave.

Modified mean field equation with a "Quantum pressure" term (*Kolomeisky-Straley 1992, Damski 2006*; see also *Kulkarni et al 2013*)

(Continuity equation is not modified)

$$\partial_t v + \partial_x(v^2/2 + \pi^2\rho^2/2 + V(x) - \frac{1}{2}\frac{\partial_x^2\sqrt{\rho}}{\sqrt{\rho}}) = 0$$

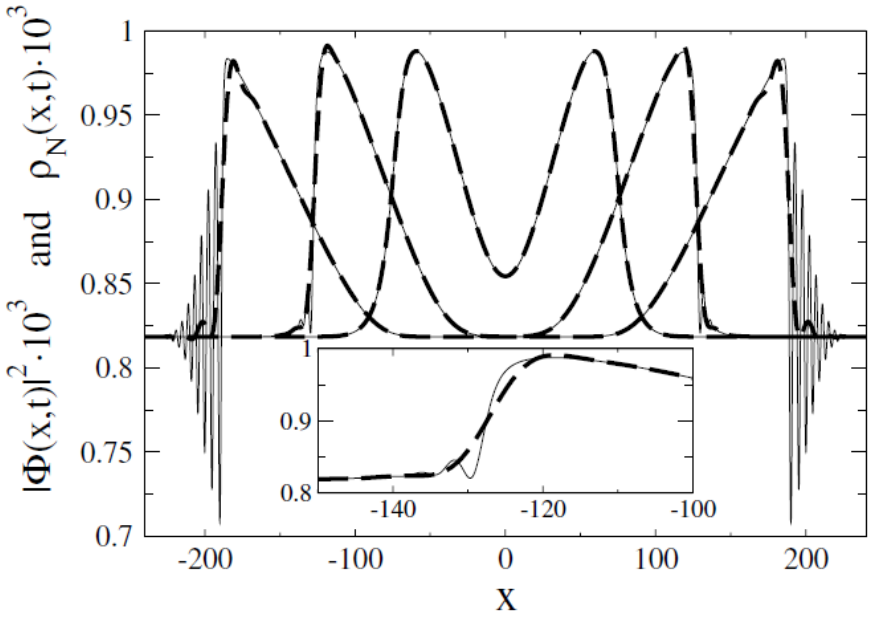

Shock formation: high compression regions propagate faster, creating a shock front.

Density of atoms as a function of time. Sequence of profiles corresponds to t = 41, 82, 131.2. Dashed line is an exact N-body calculation, while the solid line presents the numerical solution of mean-field equation. Inset shows details of a density profile at t = 82. Shock characteristics: t_c = 81.6 and x_s = 118.4.

A brief review of $c = 1$ techniques

- $c = 1$ matrix model is a matrix quantum mechanics with inverted harmonic oscillator potential. This is proposed to be a nonperturbative formulation of quantum string theory in two dimensions.

- For our purposes, we will need the fermionic formulation of the matrix quantum mechanics *Sengupta-Wadia 1990, Dhar-Mandal-Wadia 1992-1994* (see also *Mandal-Morita 2009* for application of this formalism to two-dimensional gauge theory). The eigenvalues $x_i(t)$ of the matrix behave like fermions subject to a one-body hamiltonian

$$\hat{h} = -\frac{1}{2}\hbar^2(\partial_x)^2 + V(x)$$

For the $c = 1$ model, $V = -x^2/2$, but we will allow a more general discussion.

- The large N limit of the fermionic model is defined by the limit

$$N \to \infty,\ \hbar \to 0,\ N\hbar = 1 \tag{1}$$

(the $c = 1$ model employs a 'double scaling' limit in which the depth of the fermi level below the potential maximum, μ reaches zero simultaneously with the above limit, so that $N\mu$ is held fixed. We will not consider this here).

- In this limit the states can be described in terms of the phase space density $u(x, p, t)$ which satisfy

$$u * u = u \xrightarrow{\text{large } N} u^2 = u$$

$$\int dx\ dp\ u(x, p, t) = N\hbar = 1$$

$$\partial_t u + p\partial_x u - V'(x)\partial_p u = 0 \quad \text{Euler equation in phase space}$$

Droplets

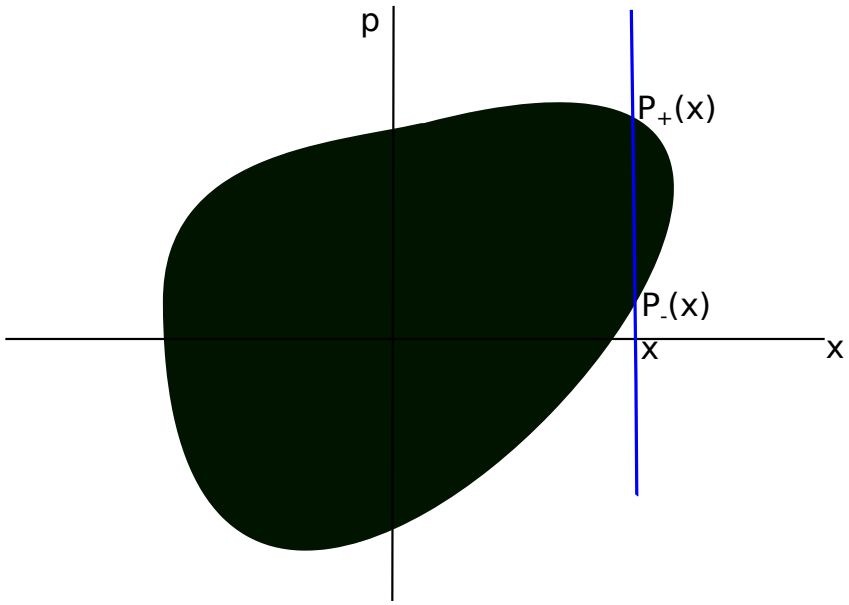

A quadratic droplet

A single connected droplet. We call it a 'quadratic droplet' if any x= constant line intersects the droplet boundary only at two points, $P_+(x)$ and $P_-(x)$. E.g. the ground state (the Fermi sea) for N fermions in a harmonic trap corresponds to a circular droplet of area $N\hbar = 1$ (in the limit (1)), with $P_\pm(x) = \pm\sqrt{\frac{1}{\pi} - x^2}$. More complicated examples of quadratic droplets can include small flucuations of such a droplet, the Fermi sea for a deformed trap etc.

For ‘quadratic droplets’, the phase space density is given by

$$u(x,p,t) = \theta\Big((P_+(x,t) - p)\Big)\theta\Big((p - P_-(x,t))\Big) \tag{2}$$

With this, the number density $\rho(x,t)$ and the specific momentum density $v(x,t)$ are given by

$$\begin{aligned} \rho(x,t) &= \frac{1}{2\pi}(P_+(x,t) - P_-(x,t)) \\ v(x,t) &= \frac{1}{2}(P_+(x,t) + P_-(x,t)) \end{aligned} \tag{3}$$

The variables $P_\pm(x,t)$ are, therefore, related to the more physical variables, the densities

$$P_\pm(x,t) = v(x,t) \pm \pi\rho(x,t)$$

It is easy to compute the total energy of a quadratic droplet (we drop the t-dependence since it is a conserved quantity)

$$\begin{aligned} H &= \int \frac{dxdp}{2\pi} h(x,p)u(x,p) \\ &= \int \frac{dx}{2\pi}\left[\frac{1}{6}\left(P_+(x,t)^3 - P_-(x,t)^3\right) + V(x)\left(P_+(x,t) - P_-(x,t)\right)\right] \\ &= \int dx\ \rho(x)(v(x)^2/2 + \pi^2\rho(x)^2/6 + V(x)) \end{aligned} \tag{4}$$

The phase space Euler equation gives two independent equations for each variable $P_\pm(x)$ (after some straightforward manipulation of the θ-functions)

$$\partial_t P_+ + \partial_x(P_+^2/2 + V(x)) = 0,\ \partial_t P_- + \partial_x(P_-^2/2 + V(x)) = 0.$$

Translated to the densities, these give the equations of conventional hydrodynamics

$$\partial_t \rho + \partial_x(\rho v) = 0$$

$$\partial_t v + \partial_x(v^2/2 + \pi^2\rho^2/2 + V(x)) = 0$$

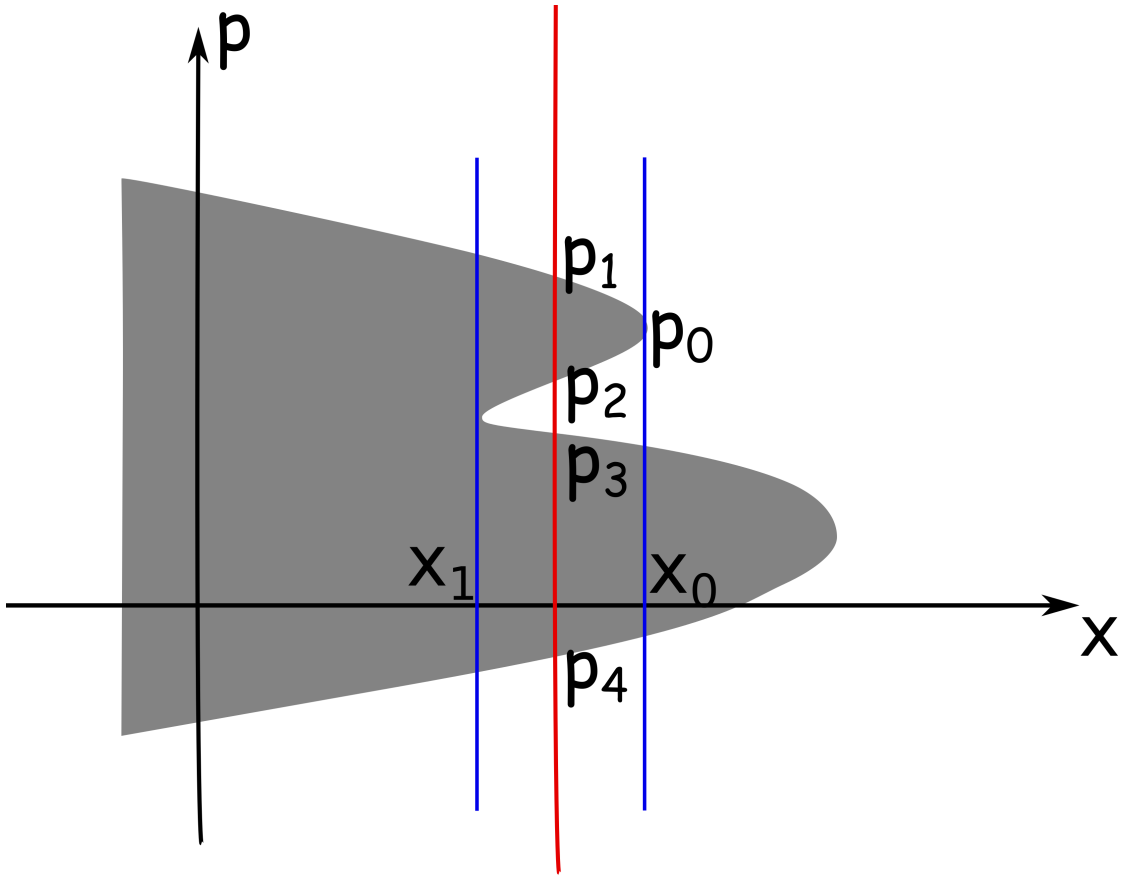

A droplet with a fold. There are values of x for which the droplet boundary $F(x, p) = 0$ has more than two roots; in the figure, there are four roots $p = p_1, p_2, p_3, p_4$. At $x = x_0$, the two roots p_1, p_2 merge: $p_1 = p_2 = p_0$. For $x > x_0$, there are only two roots p_3, p_4 and the droplet again satisfies the assumption (2) of a quadratic profile. Similarly, for $x < x_1$, only p_1, p_4 survive as real roots. In the region $x_1 < x < x_0$, the surface is said to have a 'fold'.

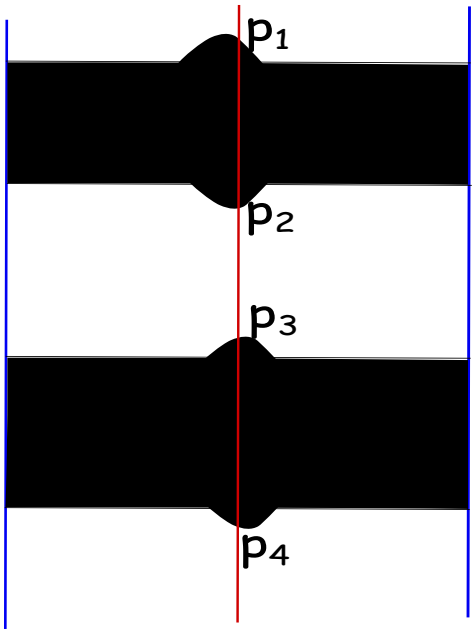

If we zoom around the red vertical line in the Figure, we would find four, apparently disconnected, fluid surfaces, somewhat like the above idealized figure. The shapes represented by the functions $p_i(x, t)$, $i = 1, 2, 3, 4$ are then in principle four independent functions. Clearly they contain more information than the two functions $\rho(x, t)$, $v(x, t)$. In fact one can imagine two independent sets of hydrodynamic variables $(\rho_{12}(x, t), v_{12}(x, t))$ and $(\rho_{34}(x, t), v_{34}(x, t))$. The actual figure above could arise as a semiclassical representation free fermions in a box in which two separate sets of momentum levels are filled and near the surface the momentum eigenstates are replaced by some localized states.

$$\rho_{12}(x,t) = \frac{1}{2\pi}\left(p_1(x,t) - p_2(x,t)\right), \qquad \rho_{34}(x,t) = \frac{1}{2\pi}\left(p_3(x,t) - p_4(x,t)\right)$$
$$v_{12}(x,t) = \frac{1}{2}\left(p_1(x,t) + p_2(x,t)\right), \qquad v_{34}(x,t) = \frac{1}{2}\left(p_3(x,t) + p_4(x,t)\right)$$
$$\rho(x,t) = \rho_{12}(x,t) + \rho_{34}(x,t), \qquad \rho(x,t)v(x,t) = \rho_{12}(x,t)v_{12}(x,t) + \rho_{34}(x,t)v_{34}(x,t)$$
$$v(x,t) = \frac{\rho_{12}(x,t)v_{12}(x,t) + \rho_{34}(x,t)v_{34}(x,t)}{\rho_{12}(x,t) + \rho_{34}(x,t)} \tag{5}$$

The density variable, at a given x appears to split into two fluid elements in the regions $p \in (p_2, p_1)$ and $p \in (p_4, p_3)$ (see the previous Figure). The variable $\rho(x,t)v(x,t)$ has a similar split; however, the velocity field does not have such a splitting.
Phase space Euler equation is local for each boundary

$$\partial_t P_i(x,t) + \partial_x (P_i(x,t)^2/2 + V(x)) = 0, \;\; i = 1, 2, \ldots, 2m-1, 2m$$

Using these equations it is easy to see that, in the presence of folds, conventional hydrodynamics equations are not satisfied.

Fluid particle description

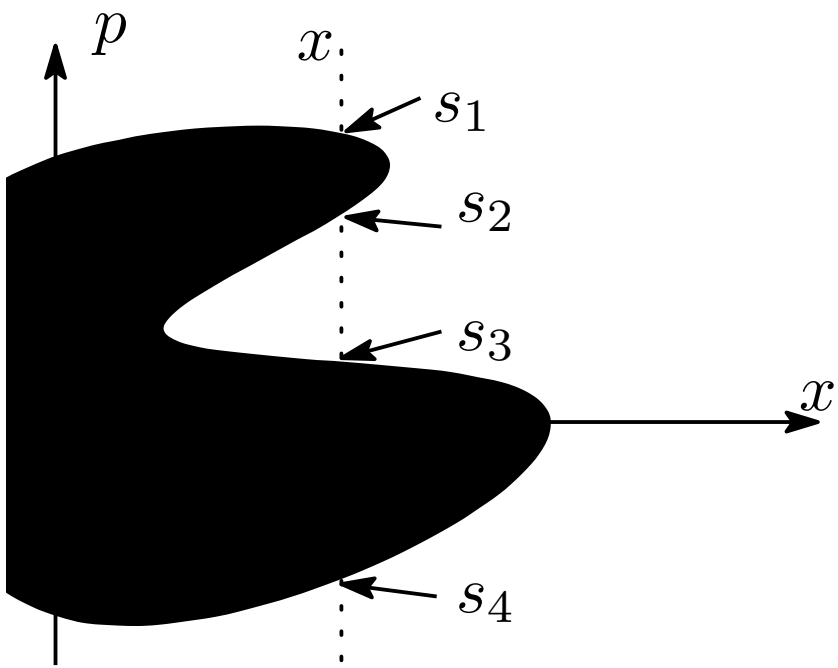

A characterization of folds in terms of the Eulerian description. We draw a vertical line corresponding to a fixed value of x. Since the fluid droplet is bounded in the vertical direction, this line may not pass through the droplet at all, or intersect the droplet boundary at an even number of points. The figure shows an example where the intersection number is four; in other words, the equation $x(s, t) = x$ has four roots s_i, $i = 1, 2, 3, 4$. This corresponds to one overhang or one 'fold' in the terminology of our paper.

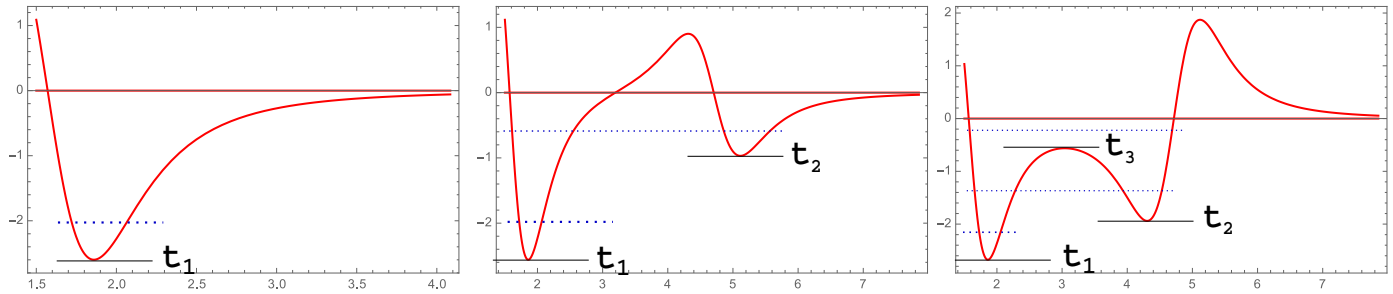

The figure shows plots of $p_0'(s)$ vs s for various initial shapes of the fluid boundary. In the left panel, $t_1 = -1/\left(p_0'(s)\right)_{\min}$. For $t < t_1$ there are no folds, whereas for $t > t_1$ the line $t = -1/p_0'$ clearly intersects the graph at two points (see the blue dotted line), hence there is one fold. In other words as the time crosses the value t_1 the number of folds grows $0 \to 1$. The behaviour of the plot above the s-axis is not relevant for this discussion for any of the plots. In the middle panel, there are two minima, we call the values of $-1/p_0'(s)$ at these two points t_1 , t_2 respectively. As time crosses t_1 and t_2 respectively, the number of folds goes $0 \to 1 \to 2$. In the right panel, there are two minima and a maximum, we call the values of $-1/p_0'(s)$ at these points t_1 , t_2 , t_3 respectively. As time crosses t_1 , t_2 and t_3 respectively, the number of folds goes $0 \to 1 \to 2 \to 1$. Note that at a maximum, two folds merge into one. In the following, we will encounter some examples of such behaviours.

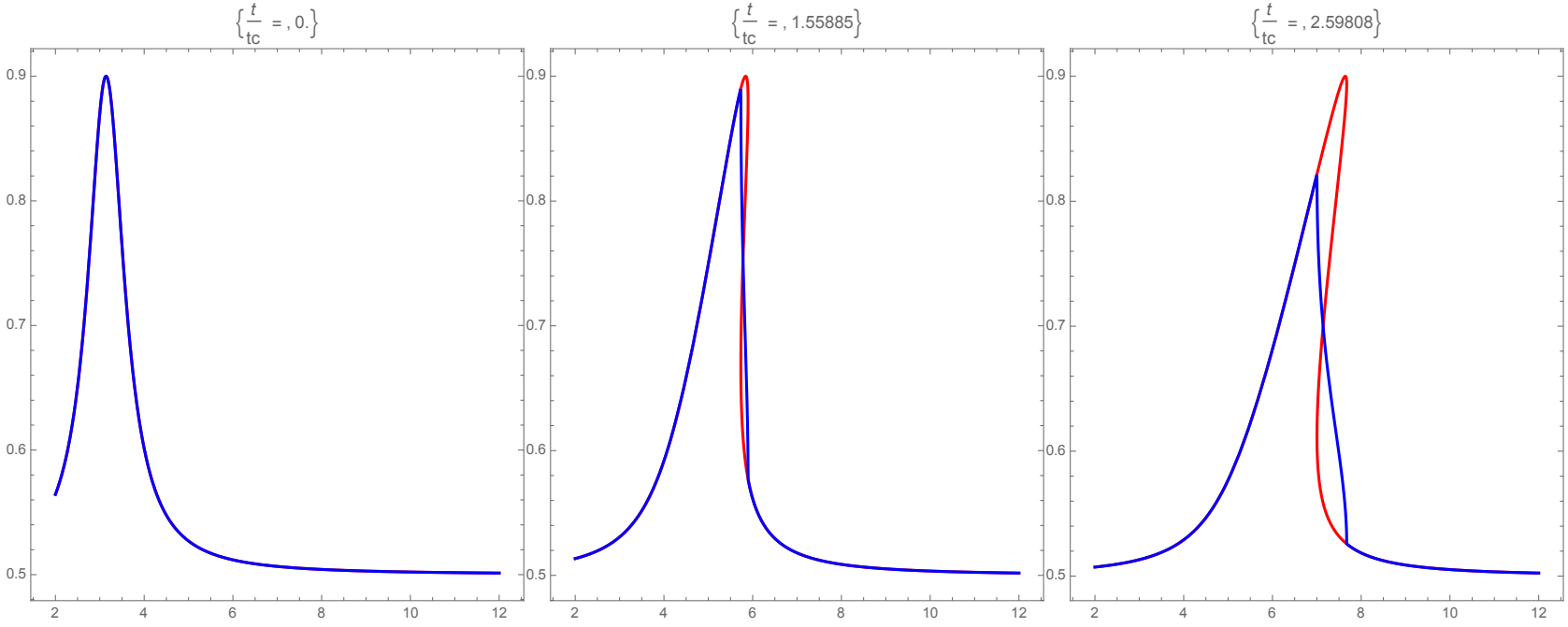

Development of a single fold: $0 \to 1$. The three panels represent snapshots at times $t = 0, 1.5t_c, 2.5t_c$ respectively, where t_c is the instant of time the overhang (fold) develops. The red curve represents (a segment of the upper part of) the fluid boundary $x = x(s, t)$, $p = p(s, t)$, while the blue curve represents the fermion density $\rho(x, t)$. The horizontal axis represents x. In the left panel, there is no overhang (no point where $\partial x/\partial s = 0$); hence $x(s, t)$ is single-valued, therefore $p(x, t)$ is single-valued, denoted by $p_+(x, t)$. Assuming that the lower boundary of the fluid profile is at $p_-(x, t) = 0$, $\rho(x, t) \equiv p_+(x, t) - p_-(x, t) = p_+(x, t)$; hence in the left panel, the blue and the red curves coincide. In the middle panel, the overhang has just developed; hence, between the two x-turning points where $\partial x/\partial s = 0$, $p(x, t)$ is multi-valued: $p_i(x, t)$, $i = 1, 2, 3$, with $\rho(x, t) = p_1 - (p_2 - p_3)$. The x-turning points lead to $\partial\rho/\partial x = \infty$ which characterize shock fronts. In the right panel, the overhang is more prominent, hence the red and blue curves are quite distinct.

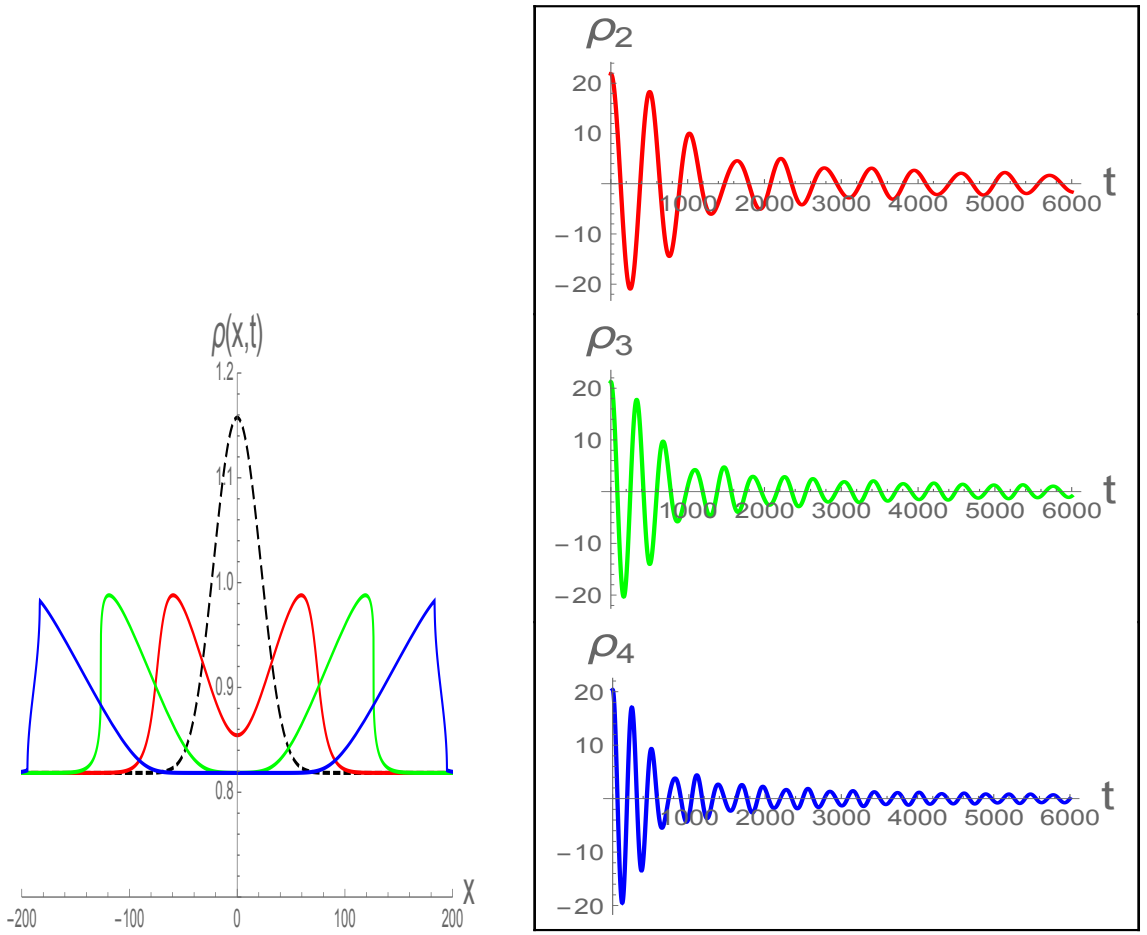

(Left Panel) Time evolution of a density profile (same as the profile of *Damski 2006* via exact field theory approach for times 0 (dashed black), 41 (red), 82 (green), 131.2 (blue). We find agreement with exact numerics. (Right Panel) Plot of various moments for the same profile.

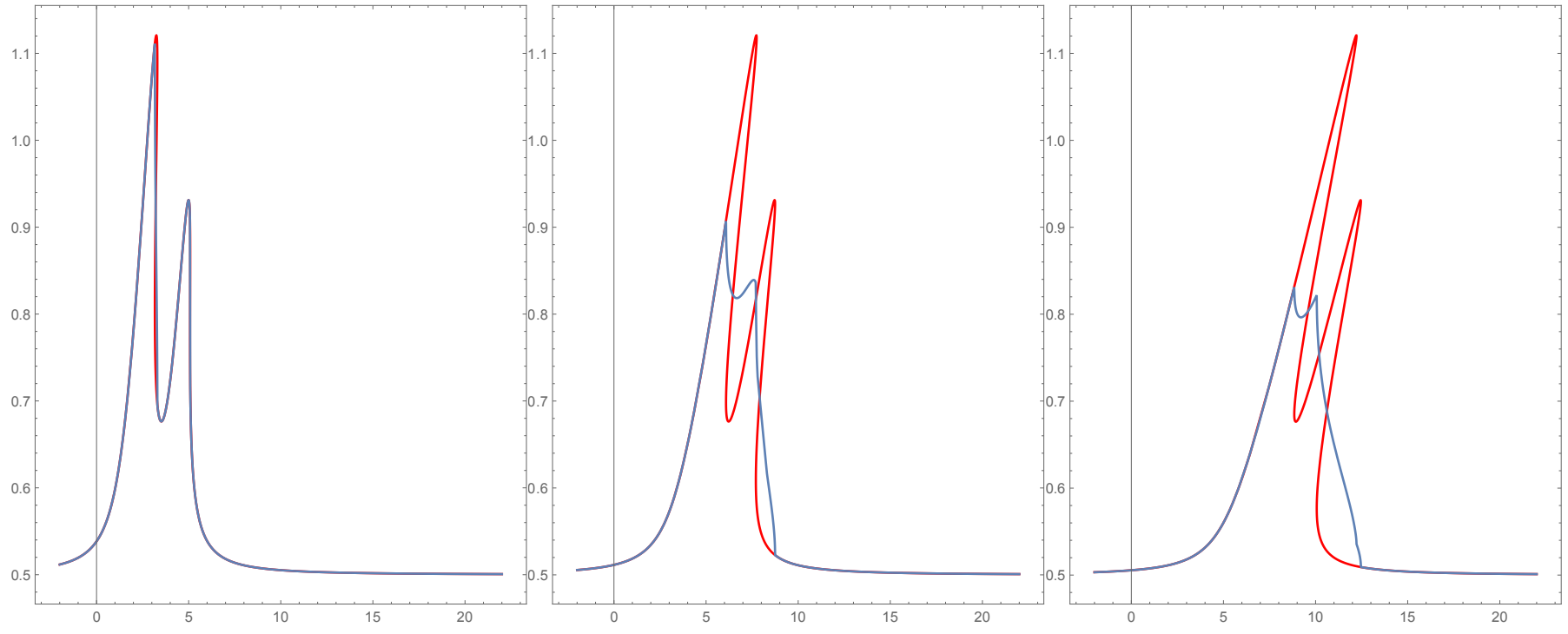

Figure : Figure for Folds $0 \to 1 \to 2$